Experimental Neurology 267 (2015) 230–242

Contents lists available at ScienceDirect

Experimental Neurology

journal homepage: www.elsevier.com/locate/yexnr

Regular Article

The secretome of apoptotic human peripheral blood mononuclear cells attenuates secondary damage following spinal cord injury in rats

Thomas Haider [a,b], Romana Höftberger [c], Beate Rüger [d], Michael Mildner [e], Roland Blumer [f], Andreas Mitterbauer [b,g], Tanja Buchacher [b,g], Camillo Sherif [h], Patrick Altmann [b,g], Heinz Redl [i], Christian Gabriel [i,j], Mariann Gyöngyösi [k], Michael B. Fischer [d,l], Gert Lubec [m], Hendrik Jan Ankersmit [b,g,*]

[a] University Clinic for Trauma Surgery, Medical University of Vienna, Währinger Gürtel 18–20, 1090 Vienna, Austria
[b] Christian Doppler Laboratory for Cardiac and Thoracic Diagnosis and Regeneration, Medical University of Vienna, Währinger Gürtel 18–20, 1090 Vienna, Austria
[c] Institute of Neurology, Medical University of Vienna, Vienna, Austria
[d] Department of Blood Group Serology and Transfusion Medicine, Medical University of Vienna, Vienna, Austria
[e] Department of Dermatology, Medical University of Vienna, Vienna, Austria
[f] Center of Anatomy and Cell Biology, Medical University Vienna, Vienna, Austria
[g] Department of Thoracic Surgery, Medical University of Vienna, Währinger Gürtel 18–20, 1090 Vienna, Austria
[h] Department of Neurosurgery, Krankenanstalt Rudolfstiftung, Vienna, Austria
[i] Ludwig Boltzmann Institute for Experimental and Clinical Traumatology, Vienna, Austria
[j] Red Cross Blood Transfusion Service of Upper Austria, Linz, Austria
[k] Department of Cardiology, Medical University of Vienna, Vienna, Austria
[l] Center for Biomedical Technology, Danube University Krems, Krems, Austria
[m] Department of Pediatrics, Medical University of Vienna, Vienna, Austria

ARTICLE INFO

Article history:
Received 16 November 2014
Revised 5 March 2015
Accepted 12 March 2015
Available online 19 March 2015

Keywords:
Spinal cord injury
Inflammation
Traumatic spinal cord injury
MNC-secretome
Oxidative stress
PBMCs
Secondary damage

ABSTRACT

After spinal cord injury (SCI), secondary damage caused by oxidative stress, inflammation, and ischemia leads to neurological deterioration. In recent years, therapeutic approaches to trauma have focused on modulating this secondary cascade. There is increasing evidence that the success of cell-based SCI therapy is due mainly to secreted factors rather than to cell implantation per se. This study investigated peripheral blood mononuclear cells as a source of factors for secretome- (MNC-secretome-) based therapy. Specifically, we investigated whether MNC-secretome had therapeutic effects in a rat SCI contusion model and its possible underlying mechanisms. Rats treated with MNC-secretome showed substantially improved functional recovery, attenuated cavity formation, and reduced acute axonal injury compared to control animals. Histological evaluation revealed higher vascular density in the spinal cords of treated animals. Immunohistochemistry showed that MNC-secretome treatment increased the recruitment of $CD68^+$ cells with concomitant reduction of oxidative stress as reflected by lower expression of inducible nitric oxide synthase. Notably, MNC-secretome showed angiogenic properties ex vivo in aortic rings and spinal cord tissue, and experiments showed that the angiogenic potential of MNC-secretome may be regulated by CXCL-1 upregulation in vivo. Moreover, systemic application of MNC-secretome activated the ERK1/2 pathway in the spinal cord. Taken together, these results indicate that factors in MNC-secretome can mitigate the pathophysiological processes of secondary damage after SCI and improve functional outcomes in rats.

© 2015 The Authors. Published by Elsevier Inc. This is an open access article under the CC BY license (http://creativecommons.org/licenses/by/4.0/).

Introduction

Injuries to the spinal cord are a devastating form of trauma that mainly affect young active patients and often result in permanent neurologic deficits, including tetraplegy (Ackery et al., 2004; Cadotte and Fehlings, 2011; Filli and Schwab, 2012). Treatment of spinal cord injury (SCI) remains challenging due to factors such as the limited potential of axonal regeneration in the human central nervous system and secondary mechanisms of injury that can last months after the initial trauma (Hall and Springer, 2004; Hausmann, 2003; Oyinbo, 2011; Popovich et al., 1997; Shechter et al., 2009; Tuszynski and Steward, 2012; Wright et al., 2011). This secondary cascade involves inflammation, neurotoxicity, glial scarring, and thrombocyte activation that, lead to micro-vascular obstruction (MVO), to injury progression, and to increased neurological impairment (Bowes and Yip, 2014; Hall and Springer, 2004; Hausmann, 2003; Kwon et al., 2004; Oyinbo, 2011;

* Corresponding author at: Department of Thoracic Surgery, Christian Doppler Laboratory for Cardiac and Thoracic Diagnosis and Regeneration, www.applied-immunology.at, Medical University of Vienna, Währinger Gürtel 18–20, A-1090 Vienna, Austria.
E-mail address: hendrik.ankersmit@meduniwien.ac.at (H.J. Ankersmit).

http://dx.doi.org/10.1016/j.expneurol.2015.03.013
0014-4886/© 2015 The Authors. Published by Elsevier Inc. This is an open access article under the CC BY license (http://creativecommons.org/licenses/by/4.0/).

Popovich et al., 1997; Rowland et al., 2008; Wright et al., 2011). Furthermore, thrombocyte activation directly promotes neuroinflammation and is involved in aggravation of neuronal damage (Joseph et al., 1991, 1992; Sotnikov et al., 2013; Thornton et al., 2010).

Despite ongoing efforts, a therapy that attenuates secondary damage after SCI has proven elusive (Cadotte and Fehlings, 2011; Filli and Schwab, 2012). Cell-based therapies using different types of stem cells, e.g. bone marrow-derived stem cells (BMSCs), looked promising in preclinical settings, but the clinical findings were not convincing (Filli and Schwab, 2012; Wright et al., 2011). In recent years, researchers have found that paracrine factors secreted by stem cells mediate the observed beneficial effects of cell therapy (Gnecchi et al., 2005; Mirotsou et al., 2011; Teixeira et al., 2013). Cantinieaux et al. reported that treatment with conditioned medium from BMSCs improves motor function and reduces spinal cord damage after SCI in rats (Cantinieaux et al., 2013). They showed that the observed therapeutic effect was due mainly to induction of angiogenesis and modulation of the inflammatory response of macrophages (Cantinieaux et al., 2013). More recently, a study reported the first use of allogeneic apoptotic cord blood MNCs in humans; these cells show regenerative potential in critical hind limb ischemia (Perotti et al., 2013). In contrast to many studies that use mesenchymal stem cells (MSCs) or other cell types, here we focused on conditioned medium from apoptotic peripheral blood mononuclear cells (PBMCs), which we term MNC-secretome. Previously we showed that MNC-secretome has regenerative effects in that it attenuates microvascular obstruction, inhibits platelets, induces vasodilation, and has immunomodulatory properties (Ankersmit et al., 2009; Hoetzenecker et al., 2012, 2015; Lichtenauer et al., 2011b; Mildner et al., 2013; Pavo et al., 2014). More recently, we demonstrated that MNC-secretome leads to reduction of infarction area in a preclinical stroke model (Altmann et al., 2014). In addition, the MNC secretome upregulates pathways associated with cytoprotection in primary neural crest-derived human cells and induces neuronal sprouting in vitro (Altmann et al., 2014). Most surprisingly, when applied intraperitoneally, the human MNC-secretome causes a huge increase in the expression of rat brain-derived neurotrophic factor (BDNF) in healthy rodents (Altmann et al., 2014). Prompted by these encouraging findings, we became interested in investigating whether MNC-secretome treatment had similar effects in a rat model of neurotrauma. Accordingly, the aim of this study was to investigate the effects of MNC-secretome treatment after SCI. For this purpose, we used a well established rat model of spinal cord contusion (Scheff et al., 2003).

Materials & methods

Ethics statement

All animal experiments were approved by the Animal Research Committee of the Medical University of Vienna (Protocol No. 66.009/0299-II/3b/2011) and met the Austrian guidelines for the use and care of laboratory animals. The local ethics committee at the Medical University of Vienna (EK2010/034) approved blood donation by healthy volunteers. All donors provided written informed consent.

Preparation of MNC-secretome

In anticipation of possible future clinical applications, we produced human apoptotic MNC-secretome according to good manufacturing practice (GMP) guidelines for all of our experiments (xenogeneic human MNCs in a rodent experimental model). Viral clearance was performed in order to comply with virus safety requirements set by national regulatory authorities.

Human MNCs were isolated from the whole blood of healthy donors by density gradient centrifugation. After 60-Gy irradiation, the cells were cultivated for 24 h with CellGro® serum-free medium without phenol red (Cellgenix, Freiburg, Germany) at a concentration of 25×10^6 cells/ml under sterile conditions. After centrifugation, the cells were discarded and the supernatant was collected. The supernatant was treated with methylene blue (MB) plus light treatment using the Theraflex MB-Plasma system (MacoPharma), the Theraflex MB-Plasma bag system (REF SDV 0001XQ), and an LED-based illumination device (MacoTronic B2, Maco-Pharma). This process is also used for production of units of fresh frozen plasma under GMP conditions (Seghatchian et al., 2011). The light energy was monitored and reached 180 J/cm^2 within 20 min of illumination time. A pill containing 85 mg of MB is integrated into the bag system, yielding a concentration range of 0.8–1.2 mmol/L MB per unit. MB and photoproducts are removed by consecutive Blueflex filtration steps; notably, a two-step filtration removes over 90% of MB (Seghatchian et al., 2011). The air was removed from the plasma units before illumination. After lyophilization of the viral-inactivated cell culture supernatant, the lyophilized powder was treated with gamma irradiation to further reduce the risk of viruses. Gamma irradiation was performed with a radioactive decay of Cobalt 60 (Gammatron 1500, Mediscan, Seibersdorf, Austria), leading to the desired sterility of the product. For this purpose, the MNC-secretome was transferred to metal sterilization boxes that pass on a meandering path through the irradiation vault around the emitting center in five layers. The cobalt unit emits photons that are almost isotropic. The dose is distributed consistently on the complex path (280 positions in 5 layers). The dose rate is recorded by a PMMA dosimeter and was determined to be 25,000 Gy after 23 h of irradiation. The lyophilized supernatant of apoptotic MNCs was considered pathogen-free after this two-step process and was stored at −80 °C until re-suspension as needed using sterile water (Aqua ad injectabilia, B Braun, Melsungen, Germany) at a concentration equivalent to 25×10^6 cells/ml. As a control, we processed CellGro® serum-free medium without phenol red in the same fashion as the cell culture supernatant. This process of producing human autologous and allogeneic MNCs was recently approved by the Austrian Health Authority.

Rats and the SCI model

Adult male Sprague Dawley rats (Department of Biomedical Research, Medical University of Vienna, Himberg, Austria) weighing 300–350 g were obtained for our experiments and housed under standard conditions with alternating 12 h light and dark cycles at the Department of Biomedical Research at the Medical University of Vienna. Standard lab chow and water was provided ad libitum. In experiments, the animals were anesthetized with 1.5% isoflurane to assure proper intraperitoneal (i.p.) application of either medium or MNC-secretome.

Contusion of the spinal cord was performed using a commercially available spinal cord impactor (Infinite Horizon Impactor, Precision System and Instrumentation, Lexington, KY) as described previously (Scheff et al., 2003). Briefly, animals were anesthetized with i.p. application of xylazine (10 mg/kg) and ketamine (100 mg/kg); anesthesia was maintained by a continuous flow of 1.5% isoflurane. Partial laminectomy to expose the spinal cord was performed at T11 under sterile conditions. The vertebral column was then stabilized by clamping the rostral and caudal vertebral bodies with Adson micro forceps (Fine Science Tools, Heidelberg, Germany). Epidural fat tissue was removed carefully while leaving the dura intact. The 2.5-mm diameter stainless steel tip was placed 1 mm above the exposed spinal cord, and a preset force of 150 kDyne was applied with instantaneous retraction of the tip, leading to a moderate contusion (Scheff et al., 2003). The exposed spinal cord was examined visually to ensure successful symmetric impact. The surgical field was irrigated with saline, and the muscle and skin openings were sutured together in layers. Animals received 10 ml of physiological saline subcutaneously (s.c.), Carprofen (10 mg/kg) s.c., and Enrofloxacin (10 mg/kg) s.c. for three consecutive days after surgery and were placed under a heating lamp during recovery. Manual bladder evacuation was performed twice daily until micturition was present. Animals were randomly divided into two groups, the Medium group and the MNC-secretome group, and received either 1 ml of processed MNC-secretome

(the equivalent of 25 × 10^6 PBMCs) or 1 ml of processed medium i.p. 40 min and 24 h after trauma. The treatment timing, frequency, and dose were determined in preliminary experiments (Altmann et al., 2014; Hoetzenecker et al., 2012; Lichtenauer et al., 2011b).

For evaluation of cytokine plasma levels 12 rats received a single i.p. dose of 1 ml containing MNC-secretome (the equivalent of 25 × 10^6 PBMCs). Plasma was taken from three rats per group sacrificed 12 h or 24 h after administration, respectively. Plasma obtained from further three untreated rats served as negative control ("0 h after treatment" in Fig. 8). (See Fig. 1.)

Functional assessment

To investigate the possible therapeutic effects of MNC-supernatant, the overground hind limb locomotion of injured rats was assessed using the Basso, Beattie, and Bresnahan 21-point open field locomotor rating scale (BBB score) (Basso et al., 1995). The score was determined before surgery (to exclude preoperative hind limb motor deficits), and 1, 3, 7, 14, 21, and 28 days after surgery. Observers were blinded with respect to treatment and previous scores. Each hind limb was scored separately, and the mean value of the scores of both limbs for each evaluation was used for statistical evaluation.

Preparation of tissue for histological and immunochemical assessment

Animals were anesthetized deeply with xylazine (10 mg/kg) i.p. and ketamine (100 mg/kg) i.p. This was followed by puncture of the inferior vena cava to draw 4 ml of blood and by euthanasia, including deep liver incision and perfusion through the heart with 20 ml of 4% paraformaldehyde in PBS. Heparin was added to the blood samples, and the samples were centrifuged at 3500*g* for 15 min. Plasma was then removed and stored at −80 °C. For histological evaluation, the vertebral column, including the spinal cord, was excised and fixed for 24 h. The spinal cord was then separated from the vertebral column, and ink marks were applied 4-mm cranial and 4-mm caudal from the injury epicenter followed by dissection of the spinal cord into an average of 10 sections. For Western blot analyses, laminectomy was performed on levels T10–T12, and around 5mm of spinal cord tissue was removed, shock frozen, and stored at −80 °C until subsequent protein extraction.

Histology and immunohistochemistry

Histological evaluation was performed on paraffin-embedded sections of spinal cords. Hematoxylin & eosin (H&E) and Luxol Fast Blue staining were performed to assess inflammation, myelin breakdown, and axonal pathology. The following were stained using immunohistochemistry: T cells (CD43/W3/13; Harlan Laboratories, Indianapolis, IN), β-amyloid precursor protein (βAPP; Chemicon International, CA), microglia/macrophages (CD68, AbDSerotec, Duesseldorf, Germany), inducible nitric oxide synthase/iNOS (Anti-NOS II, Millipore, MA), and blood vessels (anti-von Willebrand factor/vWF, Abcam, Cambridge, UK). For staining, paraffin sections were pretreated with a steamer for 60 min. The bound primary antibody was detected with a biotin–avidin technique as described in detail previously (Kerlero de Rosbo et al., 1997). To determine axonal pathology using anti-βAPP staining, comparable 0.25 mm^2 areas in the lateral column of the injured spinal cord were defined 4-mm rostral and 4-mm caudal to the injury epicenter. In this field, βAPP-positive fibers were counted using ImageJ software (Rasband, W.S., ImageJ, U.S. National Institutes of Health; Bethesda, MD). The area of cavity formation was measured in axial sections 4-mm cranial and 4-mm caudal to the injury epicenter using ImageJ planimetry software. The areas of the spinal cord section and cavity formation were measured, and their ratio was calculated. The mean values of the cranial and caudal measurements were then calculated and used for statistical evaluation. We quantified CD68 (activated microglia and macrophages), iNOS, vWF (endothelium), and CD43 (T-cells) as follows. The dorsal column and the anterolateral white matter were evaluated separately to distinguish between directly damaged and indirectly damaged spinal cord pathways. The areas and mean number of positive cells of at least 6 cross sections were counted for each animal and plotted as cell number/area. Observers blinded to treatment conducted all histological evaluations and measurements. All measurements were carried out using ImageJ.

We utilized the diaminobenzidine-enhanced Turnbull blue staining method (TBB) for the detection of non-heme iron. Ferritin expression was visualized by immunohistochemistry using rabbit anti-ferritin antibody (Sigma, St Louis, MO; dilution: 1:1000, 60 min steaming with EDTA pH 8.5). Slides were then evaluated using light microscopy. Iron accumulation was quantified by a blinded observer with the following scoring system: 0 = negative, 1 = low staining intensity, 2 = intermediate staining intensity, high staining intensity. Microglia and macrophages were distinguished by morphological appearance.

Aortic ring assay and spinal cord assay

Angiogenic activity was studied using the aortic ring assay based on the method published by Nicosia and Ottinetti (1990). Ring segments of rat aorta were sandwiched between two fibrin gels in individual wells of a 24-well culture plate (Corning, Corning, NY) and overlayed with M199 medium (Invitrogen, Carlsbad, CA) supplemented with 4 mM L-glutamine (Invitrogen), antibiotic antimycotic solution (100 U penicillin, 100 μg/ml streptomycin, 250 ng/ml amphotericin B, Sigma, St. Louis, MO) and 10% FCS (Invitrogen). Fibrin matrices were prepared as described previously with some modifications (Ruger et al., 2008). In brief, human fibrinogen (2 mg/ml, Calbiochem, Darmstadt, Germany) was dissolved in PBS supplemented with 200 U/ml aprotinin (Gerot Pharmaceutica, Vienna, Austria) to prevent fibrinolysis. Clotting was initiated by adding human plasma thrombin (0.6 U/ml, Sigma, St. Louis, MO). After equilibration, the culture medium was removed and exchanged with complete M199 without or with the addition of MNC-

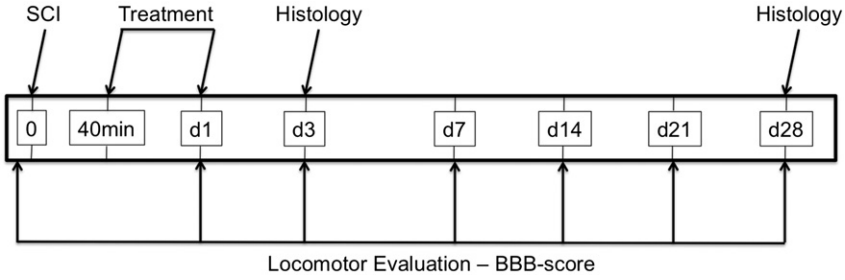

Fig. 1. Experimental timeline. Evaluation of motor function was conducted before and on days 1, 3, 7, 14, 21, and 28 after spinal cord injury (SCI). MNC-secretome or control medium was administered intraperitoneally 40 min and 24 h after SCI. Spinal cords were harvested 3 or 28 days after SCI and histological evaluation was performed. BBB score, Basso, Beattie, and Bresnahan score.

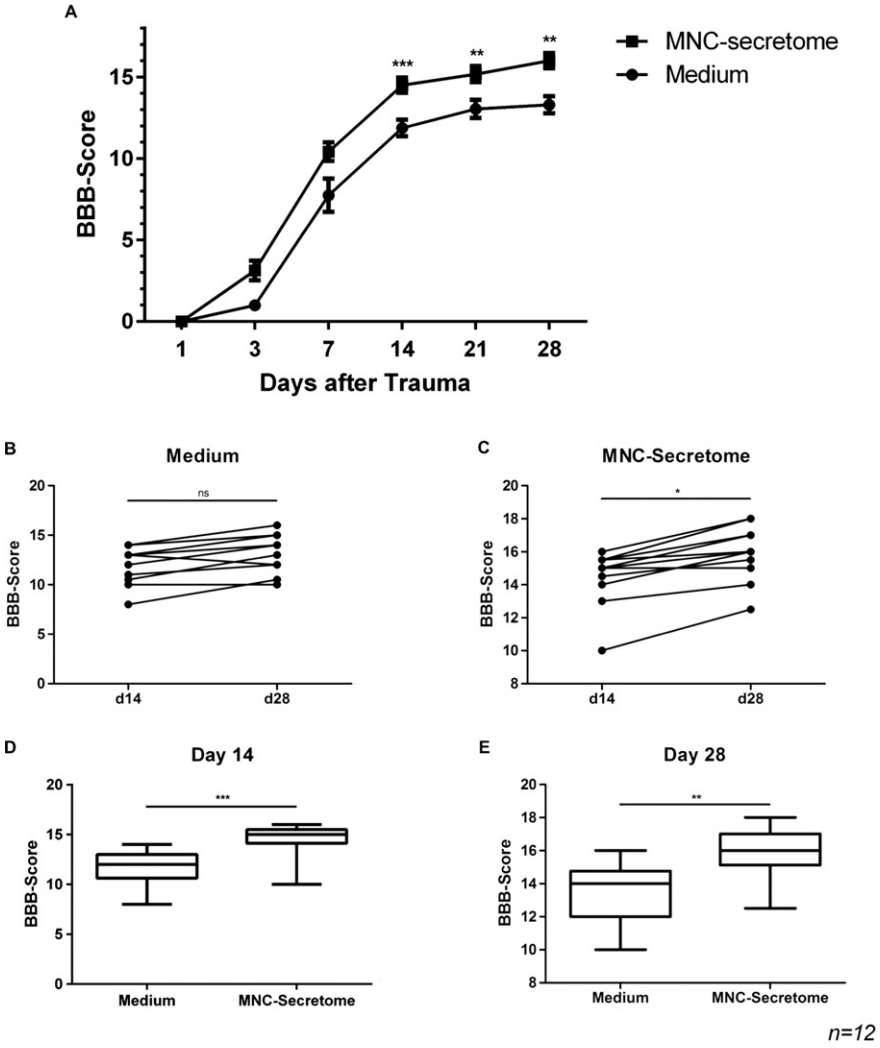

Fig. 2. Improved hind limb motor function after treatment with MNC-secretome. (A) Neurologic evaluation using the Basso, Beattie, and Bresnahan (BBB) scale revealed improved hind limb motor function at the indicated times after spinal cord injury (SCI) in animals treated with MNC-secretome as shown by the higher BBB scores (mean ± SD; Medium: d7: 7.75 ± 3.52, d14: 11.88 ± 1.76, d21: 13.04 ± 1.94, d28: 13.29 ± 1.84, MNC-secretome: d7: 10.42 ± 1.99, d14: 14.5 ± 1.62, d21: 15.17 ± 1.71, d28: 16.0 ± 1.61; Medium vs. MNC-secretome: d7: $p = 0.068$, d14: $p < 0.001$, d21: $p < 0.01$, d28: $p < 0.01$). (B,C) Improvement between day 14 and day 28 was not significant in the control group (B) (mean ± SD ; Day 14: 11.88 ± 1.76, day 28: 13.29 ± 1.84, $p = 0.07$), while in the same time period MNC-secretome treated animals experienced significant improvement in motor function (C) (mean ± SD ; Day 14: 14.50 ± 1.62, day 28: 16.00 ± 1.61, $^{*}p < 0.05$). (D, E) Comparison of day 14 (D) and day 28 (E) BBB-scores in both groups (mean ± SD; Medium vs. MNC-secretome: Day 14: 11.88 ± 1.76 vs. 14.50 ± 1.62, $^{***}p < 0.001$, day 28: 13.29 ± 1.84 vs. 16.0 ± 1.61 , $p < {}^{**}0{,}01$). n = 12 animals per group.

secretome (secretome corresponding to 4×10^6 PBMCs), MNC-secretome + anti-VEGF (300 ng/ml), recombinant rat VEGF (rrVEGF, 100 ng/ml), or rrVEGF + anti-VEGF (100 ng/ml and 300 ng/ml, respectively). The plate was incubated at 37 °C in a 5% CO2/97% humidified environment. Cultures were maintained for 4–7 days with medium changes every 2 days. The formation of tubular structures was monitored using a phase contrast microscope (Olympus IMT-2, Tokyo, Japan) on day 2, day 4, and day 6 using a digital camera (Olympus DP50). Outgrowth length was measured using ImageJ software (Rasband, W.S., ImageJ, U.S. National Institutes of Health; Bethesda, MD).

In order to quantify the cellular outgrowth from the aortic rings, the fibrin gels were dissolved as described previously (Carrion et al., 2014). The aortic rings were removed, and the remaining cells were washed with PBS and counted in a Bürker–Türk counting chamber.

To assess angiogenic capacity in the central nervous system, we used spinal cord tissue instead of aortic rings. Spinal cord segments (T1–L3) from healthy rats were embedded in 3D fibrin gels in 24-well culture plates using the same method as for the rat aortic rings. In some experiments, imaging chambers for high-resolution microscopy (ibidi, Martinsried, Germany) were used for immunofluorescence analyses and subsequent confocal laser scanning microscopy of the 3D cultures.

For flow cytometry experiments human MNCs were isolated by density gradient centrifugation and seeded in 3D fibrin cultures as described above. After six days cultures were again dissolved and processed for flow cytometry experiments.

Flow cytometry

100×10^5 cells per 100 μl PBS were stained with 10 μl PE-conjugated CD14 (clone RMO52), CD163 (clone GHI/61) and FITC-conjugated CD206 (clone 19.2) or with the appropriate isotype control antibodies (BD Biosciences) at 4 °C for 15 min. After one washing step, marker expression was analyzed on an FC 500 flow cytometer (Beckman Coulter), and data were analyzed using the FlowJo software (Tree Star Inc, Ashland, OR). Living macrophages were gated according to their forward- and side scatter characteristics and apoptotic or dead cells were excluded using the Annexin V-FITC/PI apoptosis detection kit (BD Biosciences).

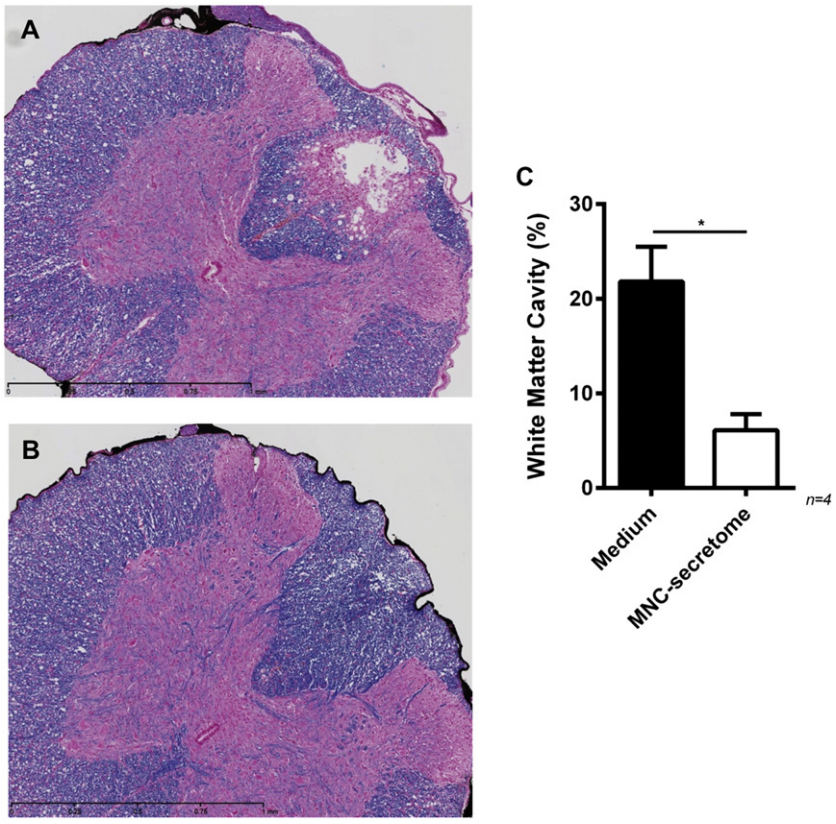

Fig. 3. Planimetric evaluation of cavity formation. Representative images of Luxol Fast Blue staining of spinal cords from (A) medium treated and (B) MNC-secretome treated animals 28 days after spinal cord injury (SCI). We marked cross sections 4-mm cranial and 4-mm caudal of the macroscopic lesion epicenter and used these for planimetric measurement. We also measured the cavity formation relative to the total dorsal column for each cross section. Then, the mean of both sections, 4-mm caudal and 4-mm cranial, was calculated for each rat and used for statistical evaluation and comparison (C; Medium vs. MNC-secretome: 21.81 ± 7.34% vs. 6.1 ± 3.4%, $^{*}p < 0.05$). n = 4 animals per group.

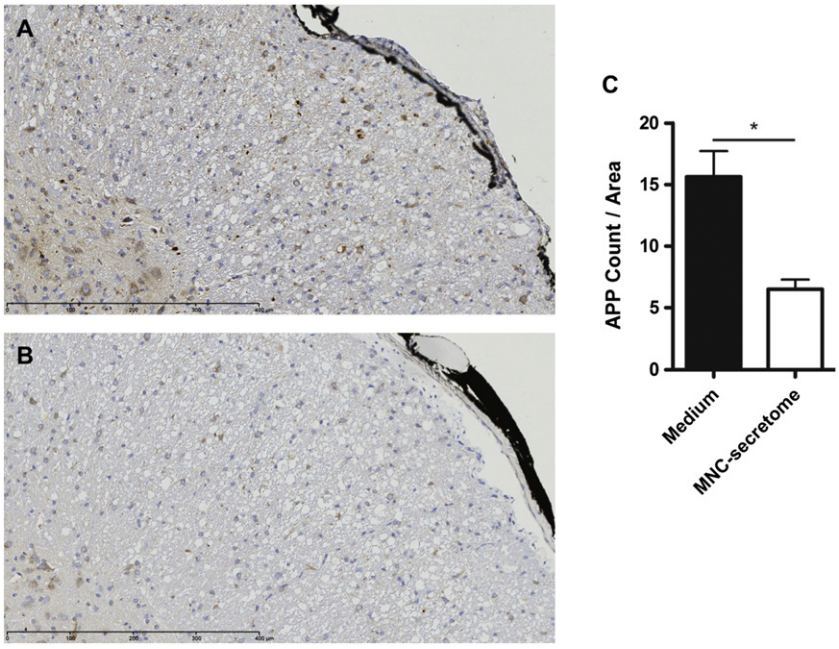

Fig. 4. Axonal damage was reduced in MNC-secretome treated animals. Immunohistochemical staining for β-amyloid precursor protein showed progressed axonal damage in spinal cord injury (SCI) animals treated with medium (A) than in animals treated with MNC-secretome (B). Similar to the method used for planimetric evaluation of lesion volume, cross sections 4-mm caudal and 4-mm cranial to the lesion epicenter were used for assessment of axonal pathology. Statistical analysis revealed significantly less in MNC-secretome treated animals, indicating reduced acute axonal injury (C; Medium vs. MNC-secretome: 16.73 ± 8.67/mm^2 vs. 6.5 ± 0.77/mm^2, $p < 0.05$). n = 5 animals per group.

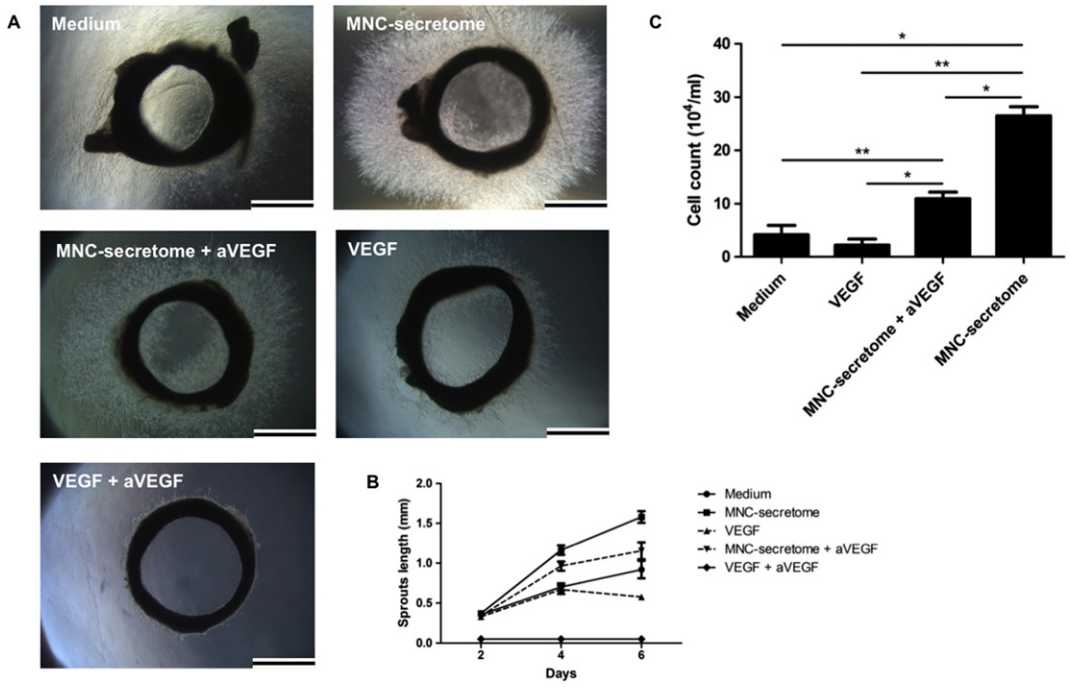

Fig. 5. Evaluation of angiogenic properties in a rat aortic ring model. (A) Representative phase contrast images of aortic rings cultured for four days in the indicated conditions: Medium, MNC-secretome, MNC-secretome + anti-VEGF, recombinant VEGF, and recombinant VEGF + anti-VEGF. (B) Graph showing the lengths of vessel sprouts on days 2, 4, and 6 after initiation of experiments. Aortic rings cultured with MNC-secretome showed the strongest angiogenic response of all groups (2-way ANOVA: MNC-secretome vs. Medium: $p < 0.001$; MNC-secretome vs. VEGF: $p < 0.001$; MNC-secretome vs. MNC-secretome + anti-VEGF: $p < 0.001$; MNC-secretome vs. recombinant VEGF + anti-VEGF: $p < 0.001$). The lengths of the 3 longest vessel sprouts were measured, and the mean length was calculated for each aortic ring and used for statistical calculations. (Mean ± SEM in mm, Day 2: MNC-secretome: 0.371 ± 0.023; Medium: 0.356 ± 0.039; VEGF: 0.328 ± 0.014; MNC-secretome + anti-VEGF: 0.340 ± 0.011; recombinant VEGF + anti-VEGF: 0.000 ± 0.000; Day 4: MNC-secretome: 1.164 ± 0.059; Medium: 0.703 ± 0.044; VEGF: 0.668 ± 0.052; MNC-secretome + anti-VEGF: 0.963 ± 0.057; recombinant VEGF + anti-VEGF: 0.000 ± 0.000; Day 6: MNC-secretome: 1.579 ± 0.073; Medium: 0.919 ± 0.109; VEGF: 0.578 ± 0.027; MNC-secretome + anti-VEGF: 1.155 ± 0.106; recombinant VEGF + anti-VEGF: 0.000 ± 0.000). (C) After ending the experiment and dissolving the assay matrix, there were significantly more cells in the MNC-secretome group compared to the other groups (MNC-secretome vs. Medium: $p < 0.05$; MNC-secretome vs. VEGF: $p < 0.01$; MNC-secretome vs. MNC-secretome + anti-VEGF: $p < 0.05$); (Means ± SEM in 10^4 cells/ml: MNC-secretome: 26.50 ± 1.71; Medium: 4.17 ± 1.75; VEGF: 2.21 ± 1.14; MNC-secretome + anti-VEGF: 10.96 ± 1.22). *$p < 0.05$, **$p < 0.01$. Scale bars, 1 mm. n = 3 per group.

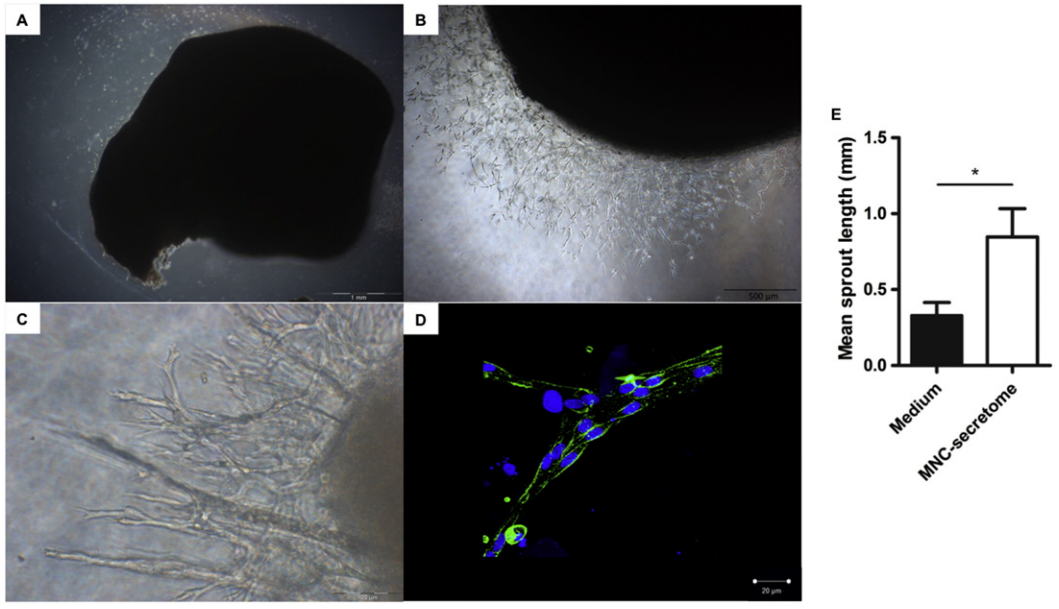

Fig. 6. Angiogenic potential of MNC-secretome in rat spinal cord tissue. (A) Representative phase contrast image of spinal cord tissue in the 3D fibrin matrix on day 6 of culture with control medium. (B, C) Representative phase contrast images of spinal cord tissue in 3D fibrin matrix on day 6 of culture with MNC-secretome. (D) Confocal laser scanning microscopy 3D-reconstruction (z-stack) of newly formed vascular sprouts in 3D fibrin matrix on day 6 of culture with MNC-secretome. The vascular structures expressed the endothelial marker RECA-1 (green). Nuclei are stained with DAPI (blue). (E): Graph showing sprout length on day 6 after initiation of 3D culture with either medium or MNC-secretome (Medium: 0.330 ± 0.084, MNC-secretome: 0.842 ± 0.186, *$p < 0.05$). Scale bars, as indicated. n = 3 per group.

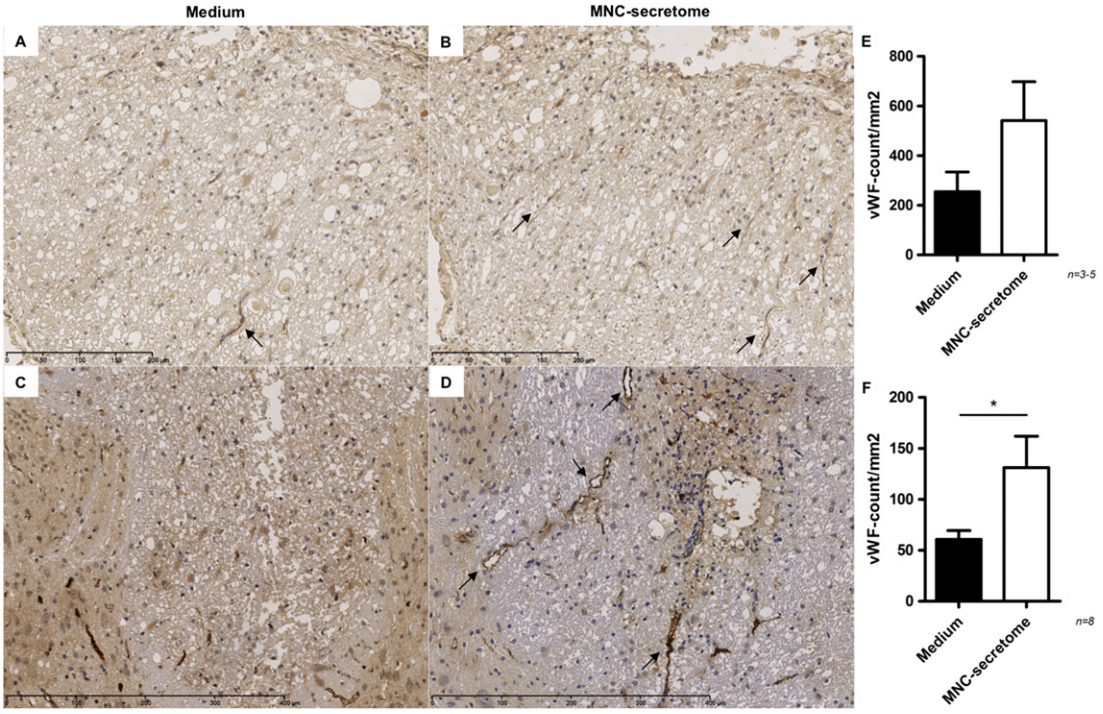

Fig. 7. MNC-secretome treatment leads to elevated expression of von Willebrand factor (vWF) in contused spinal cords. (A, B, C, D) Representative images of vWF-staining in the lesion epicenter (A, B) and in the dorsal column (C, D) 28 days after spinal cord injury (SCI) in animals treated with medium (A, C) or MNC-secretome (B, D). Arrows indicate vasculature expressing vWF. (E, F) Graphs showing the quantification of cells expressing vWF in the lesion epicenter (E) and dorsal column (F) 28 days after SCI. (Epicenter: Medium vs. MNC-secretome: 254.9 ± 78.99/mm^2 vs. 541.5 ± 156.5/mm^2, $p = 0.11$; Dorsal column: Medium vs. MNC-secretome: 60.74 ± 8.69/mm^2 vs. 131.2 ± 30.84/mm^2, $^*p < 0.05$).

Immunofluorescence and confocal laser scanning microscopy of rat spinal cord 3D cultures

To investigate the vascular phenotype of the cellular outgrowth from the rat spinal cord segments embedded in the 3D fibrin matrix, whole cultures were immunostained with RECA-1 (Abcam, Cambridge, UK), a monoclonal antibody to rat endothelial cells. 3D cultures were fixed with 4% paraformaldehyde followed by incubation with PBS/0.1 M glycine. After blocking with 5% donkey serum in immunofluorescence (IF) buffer containing 0.2% Triton X-100, 0.1% BSA, and 0.05% Tween 20 in PBS, the fibrin gel cultures were incubated with RECA-1 antibody (2 μg/ml) for 5 h at RT followed by an extended washing step with IF buffer. Visualization of the bound antibody was achieved by incubation with Alexa Fluor 488-labeled donkey anti-mouse antibody (2.5 μg/ml, Invitrogen). Cultures were washed with IF buffer, the nuclei were stained with DAPI, and the fibrin gels were stored in PBS at +4 °C until confocal laser scanning microscopy analysis. The 3D cultures were evaluated using a LSM 700 confocal laser scanning microscope (Carl Zeiss, Jena, Germany), and the acquired images were analyzed with the ZEN image processing and analysis software program (Zeiss).

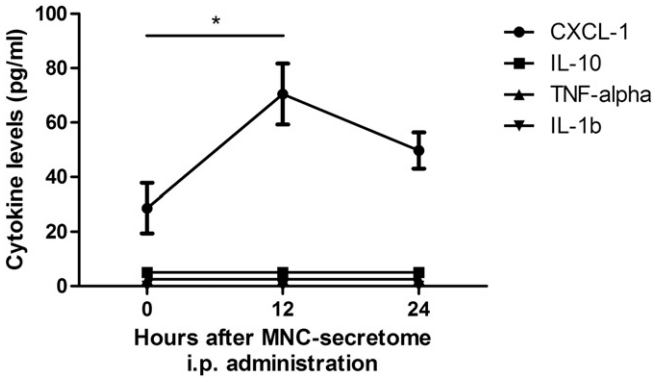

Fig. 8. Upregulation of CXCL-1 in-vivo after intraperitoneal (i.p.) administration of MNC-secretome. I.p. application of MNC-secretome increased the serum levels of CXCL-1 in healthy rats 12 h after administration compared to control animals (Medium vs. MNC-secretome: 28.63 ± 9.23 pg/ml vs. 70.5 ± 11.22 pg/ml, $^*p < 0.05$). After 24 h, the difference was not significant (Medium vs. MNC-secretome: 28.63 ± 9.23 pg/ml vs. 49.69 ± 6.65 pg/ml, $p = 0.138$). The other measured cytokines, i.e. IL-10, TNF-α, and IL-1β, were not detectable either 12 or 24 h after administration. $n = 3$ animals per group.

Western blot analysis

To analyze the phosphorylation state of intracellular signaling molecules in the spinal cord, we euthanized healthy rats 2 h after i.p. administration of either MNC-secretome or medium (control), removed the T10–T12 segments, and flash froze the segments in liquid nitrogen. Sample processing and Western blot analysis were carried out as described previously (Gschwandtner et al., 2014). Briefly, the samples were lysed in buffer containing 50 mM Tris (pH 7.4) and 2% SDS followed by sonication, centrifugation, protein concentration measurement by BCA assay (Pierce, Rockford, IL), and denaturation with 0.1 M DL-dithiothreitol (Sigma-Aldrich). We used 8–18% gradient gels for SDS-PAGE (GE-Amersham Pharmacia Biotech, Uppsala, Switzerland) for size fractionation. After electrotransferring the proteins onto nitrocellulose membranes (Bio-Rad, Hercules, CA) and subsequent Ponceau S staining, we used the following primary antibodies for immunodetection: anti-phospho-Erk 1/2 (1:1000), anti-phospho-CREB (1:1000), anti-phopsho-Hsp27 (Ser15, 1:1000), and anti-phopsho-Akt (Ser473, 1:1000) (Cell Signalling Technology, Cambridge, UK); HRP-conjugated goat anti-mouse IgG (1:10,000, Amersham, Buckinghamshire, UK); and goat anti-rabbit IgG (1:10,000, Thermo Fisher, Rockford, IL). For detecting reaction products with chemiluminescence, we used the Immun-Star Western C Substrate kit (Bio-Rad).

Quantification of band density was carried out with ImageJ and was calculated relative to specimens from untreated healthy rats.

ELISA analysis

Plasma obtained from rats was analyzed with commercially available ELISA systems (DuoSet, R&D Systems, Minneapolis). These kits specifically detect rat cytokines. All assays were performed according to the reference manual, and samples were measured in technical duplicates. We analyzed the following cytokines: CXCL-1/CINC-1, IL-10, IL-1β, and TNF-α. Optical density values were measured at 450 nm on an ELISA plate reader (Victor3 Multilabel plate reader, PerkinElmer).

Statistical methods

If not stated otherwise, data are presented as mean ± SEM. We compared motor function and data from histological evaluations (area of cavity formation, APP, CD43, and CD68) between the two groups using the nonparametric Mann–Whitney *U*-test. We used the student's *t*-test for all other statistical calculations. SPSS software (Version 21, IBM, NY) was used for all statistical calculations. Graphs were calculated and plotted with GraphPadPrism 5 (GraphPad, CA). A p-value < 0.05 was defined as the level of significance for all experiments.

Results

Treatment with MNC-secretome improves motor function after SCI

To evaluate whether application of MNC-secretome could improve motor function after SCI, the frequently used BBB-score was utilized (Basso et al., 1995). Indeed, treatment with MNC-secretome led to significant improvement of motor function compared to treatment with medium. The differences became statistically significant 14 days after SCI and remained significant until the end of the observation period on day 28 ($n = 12$; d14: $p < 0.001$, d21: $p < 0.01$, d28: $p < 0.01$; Fig. 2). A BBB score of 13 on the 21-point scale indicates that coordinated locomotion of fore and hind limbs can be frequently observed. This represents a important milestone in regeneration after SCI (Basso et al., 1995). Fourteen days after trauma, animals in the MNC-secretome treatment group exceeded this score (mean ± SD: 14.50 ± 1.62), while medium-treated animals had a score of 11.88 ± 1.76 (mean ± SD) two weeks after SCI. This difference was highly significant with a p-value < 0.001. Contrary to animals in the control group, we found significant improvement of motor function of MNC-treated animals between day 14 and day 28 post trauma ($p < 0.05$) (Figs. 2B and C).

Animals treated with MNC-secretome show reduced cavity formation and axonal damage compared to controls

To determine whether treatment with MNC-secretome resulted in reduced secondary damage after SCI, we determined the extent of injury 28 days after trauma. Specifically, we evaluated the extent of the lesion using planimetric measurements of the cavity formation relative to the total dorsal column 4-mm caudal and 4-mm cranial to the epicenter. This revealed a significantly smaller area of white matter cavity formation 28 days post-trauma in animals treated with MNC-secretome (Medium vs. MNC-secretome: 21.81 ± 7.34% vs. 6.1 ± 3.4%, $p < 0.05$) (Fig. 3).

To further evaluate the extent of acute axonal injury of motor pathways, we quantified βAPP positive axonal spheroids within the lateral column of the spinal cord. This histological evaluation showed a significant decrease in the lateral column in animals treated with MNC-secretome compared to control animals (Medium vs. MNC-secretome: 16.73 ± 8.67/mm^2 vs. 6.5 ± 0.77/mm^2, $p < 0.05$) (Fig. 4).

Finally, we investigated the state of α-motoneurons both 3 and 28 days after SCI (Supp. Figs. 4, 5). CHaT is an enzyme involved in the synthesis of the neurotransmitter acetylcholine. CHaT staining revealed pronounced damage around the lesion 3 days after injury in both groups (Supp. Fig. 4B). Interestingly, on day 28, the spinal cord appeared to be almost totally restored except for small areas of the ventral roots in both groups (Supp. Figs. 5C, D). We did not detect any differences between the two groups in terms of CHaT staining at either time point.

MNC-secretome shows angiogenic properties in aortic rings and in ex vivo spinal cord tissue

The aortic ring model is a common model for studying the angiogenic properties of drugs (Aplin et al., 2008; Nicosia and Ottinetti, 1990). In this model, we found increased vessel formation and sprouting after incubation with MNC-secretome compared to the control group (Figs. 5A, B). Furthermore, after removing the aortic ring and dissolving the matrix, cellularity was significantly higher in samples incubated with MNC-secretome (Fig. 5C). These observed effects were not VEGF-dependent; however, we noticed destabilization of the newly formed vessels on day 6 in the groups treated with anti-hVEGF (Fig. 5A and Suppl. Fig. 1). Recombinant human VEGF served as the positive control and showed less angiogenic capacity than MNC-secretome. The angiogenic capacity of rrVEGF was completely inhibited by adding the anti-VEGF antibody (Figs. 5A, B).

We designed a new assay to investigate whether MNC-secretome also exhibits these angiogenic properties in spinal cord tissue. Briefly, instead of aortic rings, we used spinal cord tissue from healthy rats in the assay. We confirmed the angiogenic effects of MNC-secretome in spinal cord tissue, similar to our findings in the aortic ring assay. Most importantly, endothelial cell outgrowth was positive for RECA-1, an endothelial cell marker (Fig. 6).

Elevated expression of vWF in injured spinal cord following treatment with MNC-secretome

These ex vivo data suggested the pro-angiogenic properties of MNC-secretome. Previous work by our group showed that MNC-secretome has other effects that can reduce damage after myocardial infarction, like vasodilation, inhibition of platelet activation, and obviation of MVO (Hoetzenecker et al., 2012). We therefore examined whether MNC-secretome might have these effects in an SCI model. We performed immunohistochemical staining against vWF to assess the microvascular density of the spinal cord (Tseliou et al., 2014; Wei et al., 2014). The vascular density was significantly increased in the entire dorsal column of the injured spinal cords of animals treated with MNC-secretome (Medium vs. MNC-secretome: 60.74 ± 8.69/mm^2 vs. 131.2 ± 30.84/mm^2, $p < 0.05$) (Figs. 7C, D). There was also increased vascular density at the lesion site, although it did not reach a statistically significant level (Medium vs. MNC-secretome: 254.9 ± 78.99/mm^2 vs. 541.5 ± 156.5/mm^2, $p = 0.11$) (Figs. 7A, B).

MNC-secretome treatment increases CXCL-1 plasma levels in vivo

To further elucidate the MNC-secretome mechanisms of action in vivo, we investigated whether plasma levels of pro-angiogenic CXCL-1, immune modulatory IL-10, and pro-inflammatory TNF-α and IL-1β were altered in healthy animals treated with MNC-secretome. We found elevated CXCL-1 plasma levels 12 h after i.p. administration, but the levels of the other cytokines were unchanged (Fig. 8). However, in the acute phase of SCI (3 days post-SCI) CXCl-1, TNF-α, and IL-1βplasma levels showed no differences compared to controls (Supp. Fig. 6).

The immune response after SCI is modulated by MNC-secretome

Monocytes and macrophages are key players in inflammatory modulation and in the resolution of inflammation after SCI (London et al., 2013;

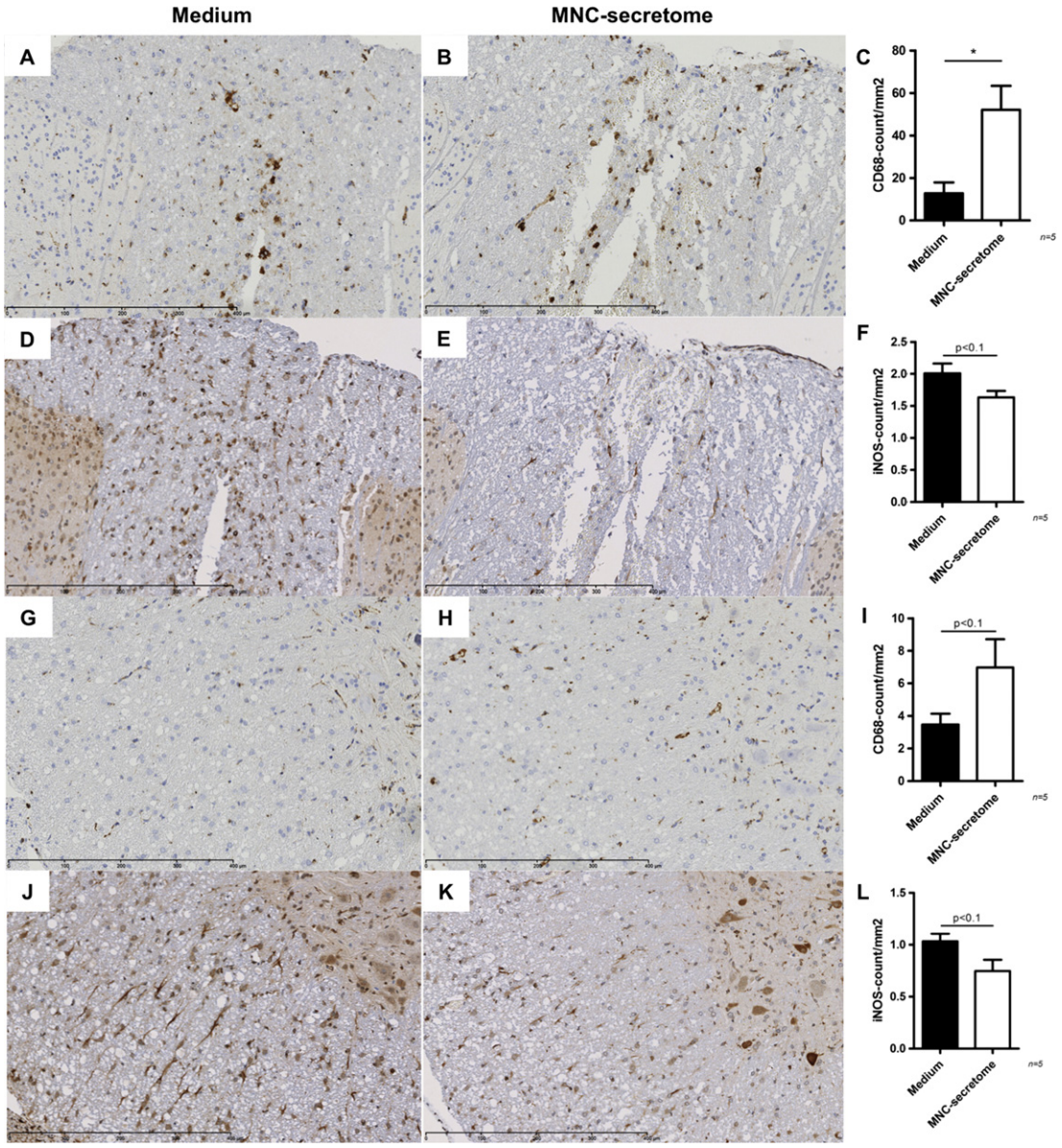

Fig. 9. Immune response after spinal cord injury is modulated by MNC-secretome. Immunohistochemical staining of the spinal cord dorsal and anterolateral columns (A, B, G, H) revealed that more cells expressed CD68 in animals treated with MNC-secretome 3 days after spinal cord injury (SCI; B, H) compared to animals treated with control medium (A, G). Despite having higher levels of $CD68^+$, tissue that was analyzed by immunohistochemistry showed lower expression levels of iNOS after treatment with MNC-secretome (E, K) compared to the spinal cord dorsal and anterolateral columns of control animals (D, J). I, J, K, L: Graphs show the number of cells expressing CD68 (C, I) and iNOS (F, L) in the dorsal and anterolateral columns of spinal cord sections (Medium vs. MNC-secretome: C: $12.7 \pm 5.2/mm^2$ vs. $52.1 \pm 11.2/mm^2$, $p < 0.05$; F: $2.0 \pm 0.2/mm^2$ vs. $1.6 \pm 0.1/mm^2$, $p = 0.072$; I: $3.5 \pm 0.7/mm^2$ vs. $6.9 \pm 1.7/mm^2$, $p = 0.097$; L: $1.0 \pm 0.1/mm^2$ vs. $0.7 \pm 0.1/mm^2$, $p = 0.061$).

Shechter et al., 2009). We were therefore interested to see whether MNC-secretome treatment modulated the immune response after SCI. Animals treated with MNC-secretome showed significantly increased $CD68^+$ cells in the dorsal column 3 days after SCI compared to controls (Figs. 9A, B, I). To assess the extent of nitric oxide radical production, we performed immunohistological staining of iNOS (London et al., 2013; Shechter et al., 2009). Despite elevated levels of $CD68^+$ cells, we found decreased iNOS expression (Figs. 9C, D, J). We observed the same trend in the remaining white matter (Figs. 9E, F, G, H, K, L). Furthermore, we detected a trend towards higher plasma levels of IL-10 on day 3 after SCI in the MNC-secretome-treated group (Supp. Fig. 2). In contrast, there were significantly higher levels of $CD68^+$ cells in the white matter of animals in the control group 28 days after SCI, while no significant differences in $CD68^+$ cell number were observed within the dorsal column (Fig. 10). We did not observe any differences in iNOS expression between the two groups 28 days after trauma (data not shown). Expression of CD43 was unaltered by MNC-secretome treatment both on day 3 and on day 28 after trauma (Supp. Fig. 3).

Augmented phosphorylation of ERK 1/2 in spinal cord tissue in response to MNC-secretome treatment

In addition to analyzing the plasma levels of a number of cytokines involved in inflammation, repair, and angiogenesis, we also investigated the activation of relevant intracellular pathways in the spinal cord after MNC-secretome treatment in healthy animals without SCI. We found a significant 2.5-fold increase in the phosphorylation of Erk 1/2 in tissue from these rats compared to tissue from untreated rats (Fig. 11B). Other pathways that we examined, including the CREB, p38, and HSP27 pathways, showed no differences in phosphorylation levels between animals treated with MNC-secretome or with medium (Fig. 11).

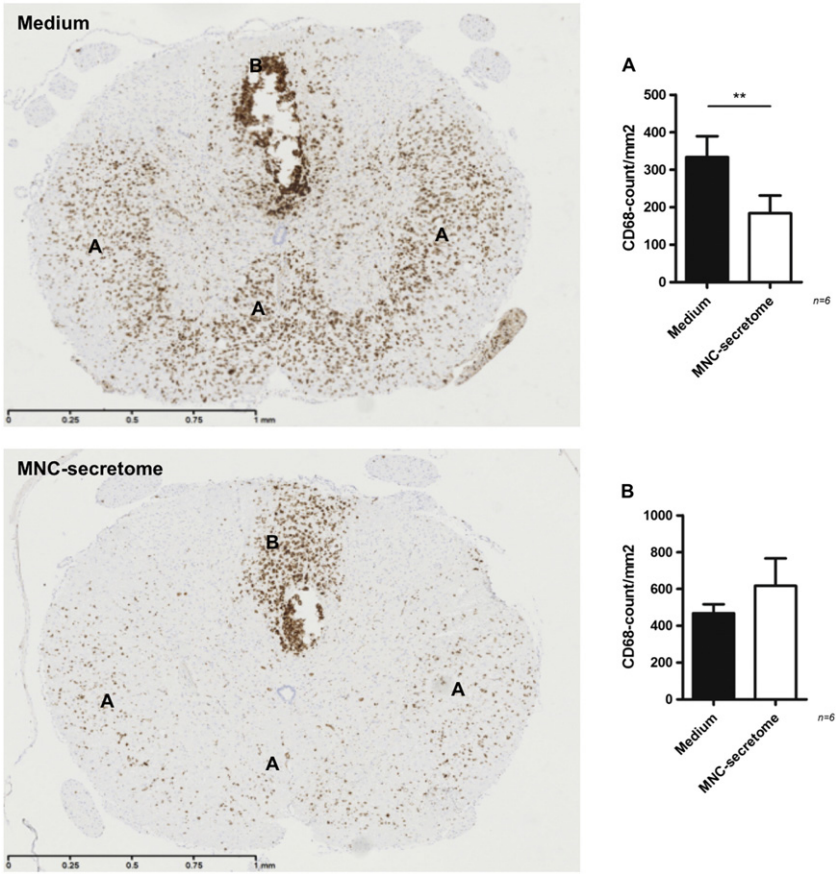

Fig. 10. CD68 expression 28 days after spinal cord injury (SCI). Representative images of immunohistological staining of CD68 in spinal cord sections 28 days after SCI. We found significantly lower expression levels of CD68 in the side and anterior columns of spinal cords after application of MNC-secretome (A; Medium vs. MNC-secretome: 333.8 ± 55.75/mm^2 vs. 183.7 ± 47.72/mm^2, **$p < 0.01$). The expression levels of CD68 were slightly higher in the dorsal column in the treatment group, although this difference was not significant (B; Medium vs. MNC-secretome: 467.1 ± 49.4/mm^2 vs. 616.9 ± 149.2/mm^2, $p = 0.21$).

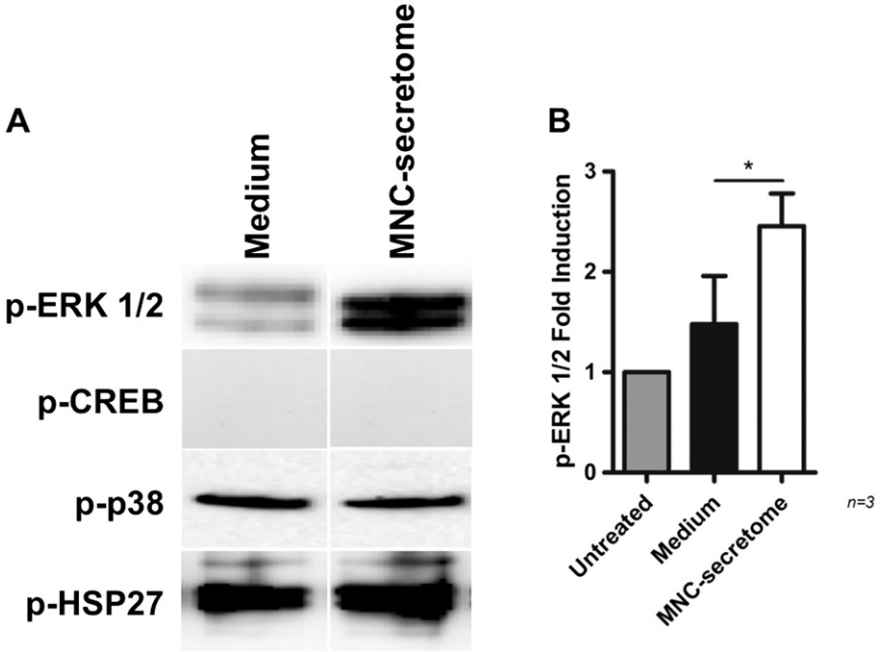

Fig. 11. MNC-secretome treatment leads to activation of the Erk-signaling cascade. Spinal cord tissue was obtained from healthy animals 2 h after i.p. treatment with either Medium or MNC-secretome. (A) Western blot analysis of the phosphorylated signaling factors pErk 1/2, pCREB, p-p38, and p-HSP27. (B) Fold increase of pErk 1/2 two hours after intraperitoneal treatment with either control medium or MNC-secretome compared to the spinal cord tissue of healthy untreated rats without spinal cord injury.

Discussion

Damage to the spinal cord following trauma can lead to permanent neurological deficits and to ongoing pain. The secondary cascade following spinal cord injury aggravates the primary lesion and exacerbates neurological impairment. This cascade elicits inflammation and ischemia, with subsequent edema formation, closing the vicious cycle (Filli and Schwab, 2012; Fleming et al., 2006; Hall and Springer, 2004; Oyinbo, 2011). Until recently, researchers in the field focused mainly on therapies that targeted mechanisms involved in this secondary cascade.

In recent years, an increasing number of studies have suggested that the immune response following SCI—apart from its detrimental effects—positively influences the outcome of this type of trauma (Bowes and Yip, 2014; London et al., 2013; Rapalino et al., 1998; Shechter et al., 2009). Suggested mechanisms include the induction of neutrophil apoptosis, the release of neurotropic factors, and axonal regrowth (Bowes and Yip, 2014; Gordon and Taylor, 2005). Improved understanding of these mechanisms made the pursuit of an effective therapy that attenuates secondary damage after SCI even more complicated and there is still a need for a multimodal therapeutic strategy.

Previously published data from our group demonstrated the regenerative properties of MNC-secretome (Hoetzenecker et al., 2012; Lichtenauer et al., 2011b; Mildner et al., 2013). The therapeutic effects of MNC-secretome include upregulation of anti-apoptotic pathways, immune system modulation, inhibition of MVO, vasodilation, and inhibition of platelet activation, all of which play major roles in secondary injury mechanisms (Filli and Schwab, 2012; Fleming et al., 2006; Hall and Springer, 2004; Hoetzenecker et al., 2012, 2015; Joseph et al., 1991, 1992; Sotnikov et al., 2013; Thornton et al., 2010). Here we utilized a commonly used spinal cord contusion injury model in rats to investigate whether the previously published characteristics of MNC-secretome are also seen in this type of injury.

The data presented here show that MNC-secretome has angiogenic potential ex vivo (Figs. 5, 6). The observed angiogenic effects were not dependent on VEGF; however, we observed destabilized vessel structures on day 6 when anti-VEGF antibody was applied along with MNC-secretome. The stabilizing and anti-apoptotic effects of VEGF on endothelial cells have been described previously and might explain vessel degradation in the absence of VEGF (Folkman and Shing, 1992; Meeson et al., 1999; Thurston and Gale, 2004). These in vitro data were corroborated by histological and morphological data evidencing increased expression of vWF in injured spinal cords after treatment with MNC-secretome compared to control 28 days after trauma (Fig. 7). We hypothesize that in addition to possible neo-angiogenesis, inhibition of MVO and subsequent reduced degradation of obliterated vessels contribute to this result. These findings confirmed published data from our group in which MNC-secretome application led to increased vessel density in a murine wound model (Mildner et al., 2013). In addition, we found increased plasma levels of pro-angiogenic rat CXCL-1 after MNC-secretome treatment of rodents (Fig. 8). CXCL-1, also known as GROα, is known for its role in angiogenesis, among other processes (Fuhler et al., 2005; Lichtenauer et al., 2012; Miyake et al., 2013). Interestingly, some data indicate that overexpression of CXCL-1 has neuroprotective effects and causes remyelination (Omari et al., 2009). A previous study reported increased plasma levels of BDNF, a key modulator in neuronal survival and differentiation, after MNC-secretome application. This mechanism was very likely involved in the therapeutic effects observed in the present study (Altmann et al., 2014; Boyd and Gordon, 2003; Song et al., 2008). Both factors, i.e. CXCL-1 and BDNF, are reported to act via the Erk 1/2 pathway (Boyd and Gordon, 2003; Fuhler et al., 2005; Miyake et al., 2013; Song et al., 2008; Wenjin et al., 2011). I.p. administration of MNC-secretome resulted in increased phosphorylation of Erk 1/2 in spinal cord tissue just one hour after application, further suggesting direct activation of this pathway by factors in the secretome (Fig. 11). Activation of the Erk 1/2 pathway was reported previously to be involved in neuroprotection (Fu et al., 2014; Toborek et al., 2007).

Because it has both detrimental and beneficial effects, the immune response following spinal cord trauma remains a difficult therapeutic target. Monocyte-derived macrophages are reported to play a central role in orchestrating the resolution of inflammation and the initiation of regenerative processes, while activation of resident microglia is thought to aggravate the injury (Rapalino et al., 1998; Shechter et al., 2009). However, due to their overlapping expression profiles, distinguishing between microglia and monocyte-derived macrophages remains challenging (London et al., 2013; Popovich and Hickey, 2001).

Consistent with previous studies, we found increased recruitment of $CD68^+$ cells to the site of injury 3 days after trauma in the MNC-secretome treated group (Fig. 9) (Lichtenauer et al., 2011b). Upregulation of iNOS, triggered by pro-inflammatory cytokines or iron accumulation via phagocytosis of erythrocytes, is thought to reflect a pro-inflammatory M1 polarization of macrophages. This M1 polarization was mainly driven and maintained by TNF expression and iron accumulation of macrophages and was detrimental to neuronal viability and neurite growth in-vitro (Bao and Liu, 2002; Hall et al., 2010; Kroner et al., 2014; Lee et al., 2014; Yune et al., 2003). To evaluate the extent of M1 macrophage polarization in our study, we evaluated the expression levels of iNOS (Gehrmann et al., 1995; Han et al., 2013). Immunostaining revealed that MNC-secretome treatment led to lower expression levels of iNOS in injured spinal cords, indicating ameliorated oxidative stress on day 3 after spinal trauma (Fig. 6). We concluded that increased CD68 expression plus concomitant reduced iNOS expression in the treatment group indicates increased recruitment of monocyte-derived macrophages. If M1 polarization of macrophages is partially driven by phagocytosis of erythrocytes and subsequent iron accumulation, presumably comparable amounts of erythrocytes in the SCI lesions phagocytized by elevated numbers of CD68-positive macrophages in the MNC-secretome-treated animals could be responsible for decreased iNOS expression and M1 polarization in individual macrophages. Evaluation of iron staining revealed lower levels of iron accumulation in animals treated with MNC-secretome supporting this hypothesis (Supp. Fig. 7). Conducting flow cytometry, we found that upon incubation with MNC-secretome human CD14 positive cells up-regulated markers associated with the immunosuppressive M2-polarization (Supp. Fig. 8) (Biswas and Mantovani, 2010; Murray and Wynn, 2011). However, this view has to be substantiated by a more detailed characterization of the possible change of macrophage phenotypes related to MNC-secretome treatment. Shechter et al. reported that the expression of IL-10 is essential for the regenerative potential of monocyte-derived macrophages after SCI (Shechter et al., 2009). Further supporting our hypothesis, we found a trend towards higher IL-10 plasma levels in MNC-secretome treated animals 3 days after spinal cord contusion (Supp. Fig. 2). On post-injury day 28, the number of CD68-positive cells was significantly lower in the MNC-secretome treatment group compared to control animals, suggesting more advanced resolution of the inflammatory response in animals treated with MNC-secretome (Fig. 10).

Taken together, these results imply that the combination of effects observed on vascularization and modulation of inflammation lead to improved motor function in MNC-secretome treated animals after SCI (Fig. 2). Surprisingly, histological evaluation revealed decreased levels of βAPP, indicating reduced axonal pathology (Fig. 4); further, lesion volume was attenuated in the treatment group, indicating that MNC-secretome reduced secondary damage after SCI (Fig. 3).

CD43 is expressed by all types of T cells, irrespective of their activation state (Clark and Baum, 2012). Previous work from our group showed that MNC-secretome has inhibitory and immune-suppressive properties and is protective against experimentally induced T-cell dependent autoimmune disease (Hoetzenecker et al., 2015). However, in this study, we did not observe any differences in CD43 expression between the MNC-secretome group and the Medium control group (Supp. Fig. 3), indicating an unaltered total number of T-cells in injured spinal cord after MNC-

secretome. This, however, does not exclude the possibility of effects of MNC-secretome treatment on the phenotype of T-cells in the setting of experimental SCI but was not further evaluated in this study.

We extended our findings by investigating differences in the ChaT staining in the treatment and control groups 3 and 28 days after trauma (Supp. Figs. 4, 5). We hypothesized that functional preservation in treated animals correlated with less acute axonal injury, as reflected by lower βAPP levels, rather than morphological recovery observable by day 28 in the ChaT staining.

Multiple previously studies have examined treatment with a single factor for complex models of disease. A study published by Lutton et al. reported the beneficial effects of the growth factors PDGF and VEGF after spinal cord hemisection in rats (Lutton et al., 2012). Interestingly, only the use of both factors together proved efficacious, while either PDGF or VEGF alone had deleterious effects that were recently confirmed in a contusion injury model (Chehrehasa et al., 2014; Lutton et al., 2012).

Here we present compelling evidence that MNC-secretome can affect multiple biological mechanisms involved in attenuating secondary damage after SCI. Both PDGF and VEGF are present in MNC-secretome and might be involved in its observed therapeutic effects (Lichtenauer et al., 2011a).

Over the years, the focus of the field of cell-based therapy has moved away from a "cell-centric" view and towards soluble paracrine factors that have observed effects in multiple pre- and clinical studies (Cantinieaux et al., 2013; Quertainmont et al., 2012; Teixeira et al., 2013; Wright et al., 2011). The first publication in the literature that supported the "paracrine hypothesis" was published in 2005 by Gnecchi et al. (2005). A recent study described the regenerative and immunomodulatory effects of the application of BMSC-conditioned medium in a SCI rat model, findings that are in accordance with our results (Cantinieaux et al., 2013).

In contrast to obtaining bone marrow stem cells and their paracrine factors, the method used to obtain MNC-secretome is simple. In previous work we showed that MNC-secretome could modulate internal inflammatory reactions in experimental stroke, acute myocardial infarction, and myocarditis (Altmann et al., 2014; Hoetzenecker et al., 2012; Hoetzenecker et al., 2015; Lichtenauer et al., 2011b).

A recent study compared the expression profiles of stem cells and MNCs (Korf-Klingebiel et al., 2008). The authors found similar cytokine concentrations in the supernatants of both cell types, with small differences in 35 of the 174 investigated secreted factors. MNCs have advantages compared to stem cells as "bioreactors" because (a) MNCs are an underutilized raw material in that currently MNCs are a waste product of the blood product generation process; (b) the secretome derived from MNCs shows minimal or no antigenicity owing to the absence of cellular epitopes; (c) MNC-secretome is easy to produce; (d) lyophilizing the conditioned medium allows "off the shelf" utilization in a clinical setting; (e) the steps involved in MNC-secretome production, including viral clearance, can be adapted to the setting of a GMP production line (which is a mandatory regulatory requirement for later clinical use in humans).

In an experimental setting, we administered the xenogenic human MNC-secretome i.p. rather than applying it locally in order to determine whether systemic application produces the desired effects found previously in experimental SCI (Abrams et al., 2012; Lee et al., 2014; Ravikumar et al., 2007). There are two possible explanations for the efficacy of systemic treatment. First, the breakdown of the blood–brain barrier after SCI allows penetration of systemic therapies; second, the systemic inflammatory response to trauma is decisive in terms of the extent of second injury (Abrams et al., 2012; Lee et al., 2014; Ravikumar et al., 2007).

Our data confirmed that the human-derived MNC-secretome attenuates secondary damage after experimental SCI. Currently we have approval from the Austrian Health Authority (AGES) to produce human allogeneic MNC secretome according to GMP guidelines, including mandatory viral clearance methods. This study provides a sound basis for the use of MNC-secretome in future SCI clinical trials.

Supplementary data to this article can be found online at http://dx.doi.org/10.1016/j.expneurol.2015.03.013.

Author disclosure statement

The Christian Doppler Research Association, APOSCIENCE AG, and the Medical University of Vienna funded this study. The Medical University of Vienna has claimed financial interest (Patent number: EP2201954, WO2010070105-A1, filed Dec 18th 2008). H.J.A. is a shareholder of APOSCIENCE AG, which owns the rights to commercialize MNC-secretome for therapeutic use. All other authors declare that they have no competing financial interest.

Acknowledgments

The authors would like to thank Irene Leißer, Gerda Ricken, Eva Dassler, Bahar Golabi and Simon Hametner for excellent technical support. The Christian Doppler Research Association provided funding for manuscript editing.

References

Abrams, M.B., Nilsson, I., Lewandowski, S.A., Kjell, J., Codeluppi, S., Olson, L., Eriksson, U., 2012. Imatinib enhances functional outcome after spinal cord injury. PLoS One 7, e38760.
Ackery, A., Tator, C., Krassioukov, A., 2004. A global perspective on spinal cord injury epidemiology. J. Neurotrauma 21, 1355–1370.
Altmann, P., Mildner, M., Haider, T., Traxler, D., Beer, L., Ristl, R., Golabi, B., Gabriel, C., Leutmezer, F., Ankersmit, H.J., 2014. Secretomes of apoptotic mononuclear cells ameliorate neurological damage in rats with focal ischemia. F1000 Research.
Ankersmit, H.J., Hoetzenecker, K., Dietl, W., Soleiman, A., Horvat, R., Wolfsberger, M., Gerner, C., Hacker, S., Mildner, M., Moser, B., Lichtenauer, M., Podesser, B.K., 2009. Irradiated cultured apoptotic peripheral blood mononuclear cells regenerate infarcted myocardium. Eur. J. Clin. Invest. 39, 445–456.
Aplin, A.C., Fogel, E., Zorzi, P., Nicosia, R.F., 2008. The aortic ring model of angiogenesis. Methods Enzymol. 443, 119–136.
Bao, F., Liu, D., 2002. Peroxynitrite generated in the rat spinal cord induces neuron death and neurological deficits. Neuroscience 115, 839–849.
Basso, D.M., Beattie, M.S., Bresnahan, J.C., 1995. A sensitive and reliable locomotor rating scale for open field testing in rats. J. Neurotrauma 12, 1–21.
Biswas, S.K., Mantovani, A., 2010. Macrophage plasticity and interaction with lymphocyte subsets: cancer as a paradigm. Nat. Immunol. 11, 889–896.
Bowes, A.L., Yip, P., 2014. Modulating inflammatory cell responses to spinal cord injury: all in good time. J. Neurotrauma 31 (21), 1753–1766.
Boyd, J.G., Gordon, T., 2003. Glial cell line-derived neurotrophic factor and brain-derived neurotrophic factor sustain the axonal regeneration of chronically axotomized motoneurons in vivo. Exp. Neurol. 183, 610–619.
Cadotte, D.W., Fehlings, M.G., 2011. Spinal cord injury: a systematic review of current treatment options. Clin. Orthop. Relat. Res. 469, 732–741.
Cantinieaux, D., Quertainmont, R., Blacher, S., Rossi, L., Wanet, T., Noel, A., Brook, G., Schoenen, J., Franzen, R., 2013. Conditioned medium from bone marrow-derived mesenchymal stem cells improves recovery after spinal cord injury in rats: an original strategy to avoid cell transplantation. PLoS One 8, e69515.
Carrion, B., Janson, I.A., Kong, Y.P., Putnam, A.J., 2014. A safe and efficient method to retrieve mesenchymal stem cells from three-dimensional fibrin gels. Tissue Eng. Part C Methods 20, 252–263.
Chehrehasa, F., Cobcroft, M., Young, Y.W., Mackay-Sim, A., Goss, B., 2014. An acute growth factor treatment that preserves function after spinal cord contusion injury. J. Neurotrauma 31 (21), 1807–1813.
Clark, M.C., Baum, L.G., 2012. T cells modulate glycans on CD43 and CD45 during development and activation, signal regulation, and survival. Ann. N. Y. Acad. Sci. 1253, 58–67.
Filli, L., Schwab, M.E., 2012. The rocky road to translation in spinal cord repair. Ann. Neurol. 72, 491–501.
Fleming, J.C., Norenberg, M.D., Ramsay, D.A., Dekaban, G.A., Marcillo, A.E., Saenz, A.D., Pasquale-Styles, M., Dietrich, W.D., Weaver, L.C., 2006. The cellular inflammatory response in human spinal cords after injury. Brain 129, 3249–3269.
Folkman, J., Shing, Y., 1992. Angiogenesis. J. Biol. Chem. 267, 10931–10934.
Fu, J., Fan, H.B., Guo, Z., Wang, Z., Li, X.D., Li, J., Pei, G.X., 2014. Salvianolic acid B attenuates spinal cord ischemia-reperfusion-induced neuronal injury and oxidative stress by activating the extracellular signal-regulated kinase pathway in rats. J. Surg. Res. 188, 222–230.
Fuhler, G.M., Knol, G.J., Drayer, A.L., Vellenga, E., 2005. Impaired interleukin-8- and GROalpha-induced phosphorylation of extracellular signal-regulated kinase result in decreased migration of neutrophils from patients with myelodysplasia. J. Leukoc. Biol. 77, 257–266.
Gehrmann, J., Matsumoto, Y., Kreutzberg, G.W., 1995. Microglia: intrinsic immuneffector cell of the brain. Brain Res. Brain Res. Rev. 20, 269–287.

Gnecchi, M., He, H., Liang, O.D., Melo, L.G., Morello, F., Mu, H., Noiseux, N., Zhang, L., Pratt, R.E., Ingwall, J.S., Dzau, V.J., 2005. Paracrine action accounts for marked protection of ischemic heart by Akt-modified mesenchymal stem cells. Nat. Med. 11, 367–368.
Gordon, S., Taylor, P.R., 2005. Monocyte and macrophage heterogeneity. Nat. Rev. Immunol. 5, 953–964.
Gschwandtner, M., Zhong, S., Tschachler, A., Mlitz, V., Karner, S., Elbe-Burger, A., Mildner, M., 2014. Fetal human keratinocytes produce large amounts of antimicrobial peptides: involvement of histone-methylation processes. J. Invest. Dermatol. 134, 2192–2201.
Hall, E.D., Springer, J.E., 2004. Neuroprotection and acute spinal cord injury: a reappraisal. NeuroRx 1, 80–100.
Hall, E.D., Vaishnav, R.A., Mustafa, A.G., 2010. Antioxidant therapies for traumatic brain injury. Neurotherapeutics 7, 51–61.
Han, H.E., Kim, T.K., Son, H.J., Park, W.J., Han, P.L., 2013. Activation of autophagy pathway suppresses the expression of iNOS, IL6 and cell death of LPS-stimulated microglia cells. Biomol. Ther. 21, 21–28.
Hausmann, O.N., 2003. Post-traumatic inflammation following spinal cord injury. Spinal Cord 41, 369–378.
Hoetzenecker, K., Assinger, A., Lichtenauer, M., Mildner, M., Schweiger, T., Starlinger, P., Jakab, A., Berenyi, E., Pavo, N., Zimmermann, M., Gabriel, C., Plass, C., Gyongyosi, M., Volf, I., Ankersmit, H.J., 2012. Secretome of apoptotic peripheral blood cells (APOSEC) attenuates microvascular obstruction in a porcine closed chest reperfused acute myocardial infarction model: role of platelet aggregation and vasodilation. Basic Res. Cardiol. 107, 292.
Hoetzenecker, K., Zimmermann, M., Hoetzenecker, W., Schweiger, T., Kollmann, D., Mildner, M., Hegedus, B., Mitterbauer, A., Hacker, S., Birner, P., Gabriel, C., Gyongyosi, M., Blyszczuk, P., Eriksson, U., Ankersmit, H.J., 2015. Mononuclear cell secretome protects from experimental autoimmune myocarditis. Eur. Heart J. 36 (11), 676–685.
Joseph, R., Tsering, C., Grunfeld, S., Welch, K.M., 1991. Platelet secretory products may contribute to neuronal injury. Stroke 22, 1448–1451.
Joseph, R., Saroff, D.M., Delfs, J.R., 1992. Platelet secretory products have a damaging effect on neurons. Neurosci. Lett. 135, 153–158.
Kerlero de Rosbo, N., Hoffman, M., Mendel, I., Yust, I., Kaye, J., Bakimer, R., Flechter, S., Abramsky, O., Milo, R., Karni, A., Ben-Nun, A., 1997. Predominance of the autoimmune response to myelin oligodendrocyte glycoprotein (MOG) in multiple sclerosis: reactivity to the extracellular domain of MOG is directed against three main regions. Eur. J. Immunol. 27, 3059–3069.
Korf-Klingebiel, M., Kempf, T., Sauer, T., Brinkmann, E., Fischer, P., Meyer, G.P., Ganser, A., Drexler, H., Wollert, K.C., 2008. Bone marrow cells are a rich source of growth factors and cytokines: implications for cell therapy trials after myocardial infarction. Eur. Heart J. 29, 2851–2858.
Kroner, A., Greenhalgh, A.D., Zarruk, J.G., Passos Dos Santos, R., Gaestel, M., David, S., 2014. TNF and increased intracellular iron alter macrophage polarization to a detrimental M1 phenotype in the injured spinal cord. Neuron 83, 1098–1116.
Kwon, B.K., Tetzlaff, W., Grauer, J.N., Beiner, J., Vaccaro, A.R., 2004. Pathophysiology and pharmacologic treatment of acute spinal cord injury. Spine J. 4, 451–464.
Lee, J.Y., Maeng, S., Kang, S.R., Choi, H.Y., Oh, T.H., Ju, B.G., Yune, T.Y., 2014. Valproic acid protects motor neuron death by inhibiting oxidative stress and endoplasmic reticulum stress-mediated cytochrome C release after spinal cord injury. J. Neurotrauma 31, 582–594.
Lichtenauer, M., Mildner, M., Baumgartner, A., Hasun, M., Werba, G., Beer, L., Altmann, P., Roth, G., Gyongyosi, M., Podesser, B.K., Ankersmit, H.J., 2011a. Intravenous and intramyocardial injection of apoptotic white blood cell suspensions prevents ventricular remodelling by increasing elastin expression in cardiac scar tissue after myocardial infarction. Basic Res. Cardiol. 106, 645–655.
Lichtenauer, M., Mildner, M., Hoetzenecker, K., Zimmermann, M., Podesser, B.K., Sipos, W., Berenyi, E., Dworschak, M., Tschachler, E., Gyongyosi, M., Ankersmit, H.J., 2011b. Secretome of apoptotic peripheral blood cells (APOSEC) confers cytoprotection to cardiomyocytes and inhibits tissue remodelling after acute myocardial infarction: a preclinical study. Basic Res. Cardiol. 106, 1283–1297.
Lichtenauer, M., Mildner, M., Werba, G., Beer, L., Hoetzenecker, K., Baumgartner, A., Hasun, M., Nickl, S., Mitterbauer, A., Zimmermann, M., Gyongyosi, M., Podesser, B.K., Klepetko, W., Ankersmit, H.J., 2012. Anti-thymocyte globulin induces neoangiogenesis and preserves cardiac function after experimental myocardial infarction. PLoS One 7, e52101.
London, A., Cohen, M., Schwartz, M., 2013. Microglia and monocyte-derived macrophages: functionally distinct populations that act in concert in CNS plasticity and repair. Front. Cell. Neurosci. 7, 34.
Lutton, C., Young, Y.W., Williams, R., Meedeniya, A.C., Mackay-Sim, A., Goss, B., 2012. Combined VEGF and PDGF treatment reduces secondary degeneration after spinal cord injury. J. Neurotrauma 29, 957–970.
Meeson, A.P., Argilla, M., Ko, K., Witte, L., Lang, R.A., 1999. VEGF deprivation-induced apoptosis is a component of programmed capillary regression. Development 126, 1407–1415.
Mildner, M., Hacker, S., Haider, T., Gschwandtner, M., Werba, G., Barresi, C., Zimmermann, M., Golabi, B., Tschachler, E., Ankersmit, H.J., 2013. Secretome of peripheral blood mononuclear cells enhances wound healing. PLoS One 8, e60103.
Mirotsou, M., Jayawardena, T.M., Schmeckpeper, J., Gnecchi, M., Dzau, V.J., 2011. Paracrine mechanisms of stem cell reparative and regenerative actions in the heart. J. Mol. Cell. Cardiol. 50, 280–289.
Miyake, M., Goodison, S., Urquidi, V., Gomes Giacoia, E., Rosser, C.J., 2013. Expression of CXCL1 in human endothelial cells induces angiogenesis through the CXCR2 receptor and the ERK1/2 and EGF pathways. Lab. Invest. 93, 768–778.
Murray, P.J., Wynn, T.A., 2011. Protective and pathogenic functions of macrophage subsets. Nat. Rev. Immunol. 11, 723–737.
Nicosia, R.F., Ottinetti, A., 1990. Growth of microvessels in serum-free matrix culture of rat aorta. A quantitative assay of angiogenesis in vitro. Lab. Invest. 63, 115–122.
Omari, K.M., Lutz, S.E., Santambrogio, L., Lira, S.A., Raine, C.S., 2009. Neuroprotection and remyelination after autoimmune demyelination in mice that inducibly overexpress CXCL1. Am. J. Pathol. 174, 164–176.
Oyinbo, C.A., 2011. Secondary injury mechanisms in traumatic spinal cord injury: a nugget of this multiply cascade. Acta Neurobiol. Exp. 71, 281–299.
Pavo, N., Zimmermann, M., Pils, D., Mildner, M., Petrasi, Z., Petnehazy, O., Fuzik, J., Jakab, A., Gabriel, C., Sipos, W., Maurer, G., Gyongyosi, M., Ankersmit, H.J., 2014. Long-acting beneficial effect of percutaneously intramyocardially delivered secretome of apoptotic peripheral blood cells on porcine chronic ischemic left ventricular dysfunction. Biomaterials 35, 3541–3550.
Perotti, C., Arici, V., Cervio, M., Del Fante, C., Calliada, F., Gnecchi, M., Ciuffreda, M.C., Scudeller, L., Bozzani, A., Ragni, F., Viarengo, G., Cervio, E., Odero, A., Redi, C.A., 2013. Allogeneic lethally irradiated cord blood mononuclear cells in no-option critical limb ischemia: a "box of rain". Stem Cells Dev. 22, 2806–2812.
Popovich, P.G., Hickey, W.F., 2001. Bone marrow chimeric rats reveal the unique distribution of resident and recruited macrophages in the contused rat spinal cord. J. Neuropathol. Exp. Neurol. 60, 676–685.
Popovich, P.G., Wei, P., Stokes, B.T., 1997. Cellular inflammatory response after spinal cord injury in Sprague–Dawley and Lewis rats. J. Comp. Neurol. 377, 443–464.
Quertainmont, R., Cantinieaux, D., Botman, O., Sid, S., Schoenen, J., Franzen, R., 2012. Mesenchymal stem cell graft improves recovery after spinal cord injury in adult rats through neurotrophic and pro-angiogenic actions. PLoS One 7, e39500.
Rapalino, O., Lazarov-Spiegler, O., Agranov, E., Velan, G.J., Yoles, E., Fraidakis, M., Solomon, A., Gepstein, R., Katz, A., Belkin, M., Hadani, M., Schwartz, M., 1998. Implantation of stimulated homologous macrophages results in partial recovery of paraplegic rats. Nat. Med. 4, 814–821.
Ravikumar, R., McEwen, M.L., Springer, J.E., 2007. Post-treatment with the cyclosporin derivative, NIM811, reduced indices of cell death and increased the volume of spared tissue in the acute period following spinal cord contusion. J. Neurotrauma 24, 1618–1630.
Rowland, J.W., Hawryluk, G.W., Kwon, B., Fehlings, M.G., 2008. Current status of acute spinal cord injury pathophysiology and emerging therapies: promise on the horizon. Neurosurg. Focus 25, E2.
Ruger, B.M., Breuss, J., Hollemann, D., Yanagida, G., Fischer, M.B., Mosberger, I., Chott, A., Lang, I., Davis, P.F., Hocker, P., Dettke, M., 2008. Vascular morphogenesis by adult bone marrow progenitor cells in three-dimensional fibrin matrices. Differentiation 76, 772–783.
Scheff, S.W., Rabchevsky, A.G., Fugaccia, I., Main, J.A., Lumpp Jr., J.E., 2003. Experimental modeling of spinal cord injury: characterization of a force-defined injury device. J. Neurotrauma 20, 179–193.
Seghatchian, J., Struff, W.G., Reichenberg, S., 2011. Main properties of the THERAFLEX MB-plasma system for pathogen reduction. Transfus. Med. Hemother. 38, 55–64.
Shechter, R., London, A., Varol, C., Raposo, C., Cusimano, M., Yovel, G., Rolls, A., Mack, M., Pluchino, S., Martino, G., Jung, S., Schwartz, M., 2009. Infiltrating blood-derived macrophages are vital cells playing an anti-inflammatory role in recovery from spinal cord injury in mice. PLoS Med. 6, e1000113.
Song, X.Y., Li, F., Zhang, F.H., Zhong, J.H., Zhou, X.F., 2008. Peripherally-derived BDNF promotes regeneration of ascending sensory neurons after spinal cord injury. PLoS One 3, e1707.
Sotnikov, I., Veremeyko, T., Starossom, S.C., Barteneva, N., Weiner, H.L., Ponomarev, E.D., 2013. Platelets recognize brain-specific glycolipid structures, respond to neurovascular damage and promote neuroinflammation. PLoS One 8, e58979.
Teixeira, F.G., Carvalho, M.M., Sousa, N., Salgado, A.J., 2013. Mesenchymal stem cells secretome: a new paradigm for central nervous system regeneration? Cell. Mol. Life Sci. 70, 3871–3882.
Thornton, P., McColl, B.W., Greenhalgh, A., Denes, A., Allan, S.M., Rothwell, N.J., 2010. Platelet interleukin-1alpha drives cerebrovascular inflammation. Blood 115, 3632–3639.
Thurston, G., Gale, N.W., 2004. Vascular endothelial growth factor and other signaling pathways in developmental and pathologic angiogenesis. Int. J. Hematol. 80, 7–20.
Toborek, M., Son, K.W., Pudelko, A., King-Pospisil, K., Wylegala, E., Malecki, A., 2007. ERK 1/2 signaling pathway is involved in nicotine-mediated neuroprotection in spinal cord neurons. J. Cell. Biochem. 100, 279–292.
Tseliou, E., de Couto, G., Terrovitis, J., Sun, B., Weixin, L., Marban, L., Marban, E., 2014. Angiogenesis, cardiomyocyte proliferation and anti-fibrotic effects underlie structural preservation post-infarction by intramyocardially-injected cardiospheres. PLoS One 9, e88590.
Tuszynski, M.H., Steward, O., 2012. Concepts and methods for the study of axonal regeneration in the CNS. Neuron 74, 777–791.
Wei, L., Zhang, J., Xiao, X.B., Mai, H.X., Zheng, K., Sun, W.L., Wang, L., Liang, F., Yang, Z.L., Liu, Y., Wang, Y.Q., Li, Z.F., Wang, J.N., Zhang, W.J., You, H., 2014. Multiple injections of human umbilical cord-derived mesenchymal stromal cells through the tail vein improve microcirculation and the microenvironment in a rat model of radiation myelopathy. J. Transl. Med. 12, 246.
Wenjin, W., Wenchao, L., Hao, Z., Feng, L., Yan, W., Wodong, S., Xianqun, F., Wenlong, D., 2011. Electrical stimulation promotes BDNF expression in spinal cord neurons through Ca(2+)- and Erk-dependent signaling pathways. Cell. Mol. Neurobiol. 31, 459–467.
Wright, K.T., El Masri, W., Osman, A., Chowdhury, J., Johnson, W.E., 2011. Concise review: bone marrow for the treatment of spinal cord injury: mechanisms and clinical applications. Stem Cells 29, 169–178.
Yune, T.Y., Chang, M.J., Kim, S.J., Lee, Y.B., Shin, S.W., Rhim, H., Kim, Y.C., Shin, M.L., Oh, Y.J., Han, C.T., Markelonis, G.J., Oh, T.H., 2003. Increased production of tumor necrosis factor-alpha induces apoptosis after traumatic spinal cord injury in rats. J. Neurotrauma 20, 207–219.